

Corrosion Behavior of Composite Coatings Obtained by Electrolytic Codeposition of Copper with Al₂O₃ Nanoparticles

I. Zamblau,^a S. Varvara,^b C. Bulea,^c and L. M. Muresan^{a,*}

^a“Babes-Bolyai” University, Department of Physical Chemistry, 11 Arany Janos St., 400028 Cluj-Napoca, Romania

^b“1 Decembrie 1918” University Alba-Iulia, Department of Topography, 11–13 Nicolae Iorga St., 510009 Alba-Iulia, Romania

^cBETAK S.A., 4 Industriilor St., Bistrita, Romania

Original scientific paper

Received: June 26, 2008

Accepted: September 4, 2008

Composite coatings of copper incorporating Al₂O₃ nanoparticles electrodeposited on carbon steel were obtained and characterized. By using electrochemical methods such as open circuit potential (*ocp*) measurements, polarization curves and electrochemical impedance spectroscopy, the corrosion behavior of the Al₂O₃-copper nanocomposite coatings was examined.

The corrosion parameters determined from the polarization curves recorded in Na₂SO₄ solution (pH 3) indicate that the corrosion process on copper-Al₂O₃ composite surface is slower than on pure copper.

The impedance spectra recorded at the *ocp* showed in all cases an increase of the polarization resistance in time, which may be explained by the development of corrosion products on the electrode surface. Using a (2RC) equivalent electrical circuit, the process parameters were estimated by non-linear regression calculations with a Simplex method. The Al₂O₃ particles embedded in the electrodeposited copper, increase the polarization resistance and decrease the corrosion rates as compared with electrodeposited pure copper.

The electrochemical results were corroborated with those obtained by SEM and EDX investigations.

Key words:

Corrosion, electrolytic codeposition, copper composite coating, Al₂O₃ nanoparticles, electrochemical impedance spectroscopy, SEM-EDX

Introduction

Metal matrix composites are attractive materials due to their properties such as increased hardness and wear resistance, low coefficients of thermal expansion, dry lubrication properties and better corrosion resistance as compared with pure metallic coatings.¹

There is a large number of useful metal/particles combinations, including metals like copper,^{2–3} nickel,^{4–6} silver,^{7–9} zinc^{10–11} and inert materials such as oxides,^{12–13} carbides,^{14–15} graphite,¹⁶ polytetrafluoroethylene (PTFE),¹⁷ etc. which are successfully used in many practical applications such as advanced surface finishing, electronic industry etc.

The methods generally used to obtain composite metallic coatings are (i) thermal methods (spray, internal oxidation); (ii) sol-gel method (hydrolysis of metallic alcoxides followed by polycondensation); (iii) dip coating or (iv) electrolytic codeposition, in direct or pulsed current.

The preparation of composite metallic layers by electrochemical methods is intensely studied, the tendency being to replace the micro-particles (used in the '90s) with nanoparticles, conferring improved properties to metallic coatings. The different electrodeposition techniques allow the obtaining of various types of nanostructured materials, ranging from single metal to alloy nanocomposites and from monolayers to multilayered deposits, through galvanostatic or potentiostatic methods.

Electrolytic codeposition presents some advantages over other methods:¹⁸ (i) the possibility of rigorous control of the deposited layer thickness; (ii) the control of deposition speed; (iii) work at room temperature, and (iv) the use of accessible equipments. By using the electrical current, the electrodeposition is suitable for obtaining non-uniform films on substrates with complex shapes (*e.g.* deposition only on some surfaces of the substrate, deposition on porous profiles etc.). At the same time, the composite deposits obtained by electrolytic methods present improved corrosion resistance as compared to the usual metallic layers, better mechanical and tribological properties.

*Corresponding author: limur@chem.ubbcluj.ro;
Tel. + 40-264-595872; Fax: + 40-264-590818

Copper composites are key electrical conductive materials used in switches for high voltage power supply appliances and in many microelectronic applications.¹⁹ With the development of portable electronic devices, copper is increasingly more exposed to corrosive conditions, and different solutions have been proposed for increasing its corrosion resistance. Thus, it was already reported that small quantities of alumina particles embedded in the copper coatings strongly improve the yield strength and hardness of deposits, their creep and arc erosion resistance at elevated temperatures, as well as their corrosion resistance without affecting the electrical and thermal conductivities.^{20–23} This is why alumina-reinforced copper matrix composite has been considered one of the best candidates for a variety of applications, including its use as hard and wear-resistant coatings for electrical contacts.^{24–27}

It should also be mentioned that, for fundamental studies, copper and Al_2O_3 can be used as a model system for the mechanistic study of particle deposition with a metallic matrix.²⁸

Nevertheless, there are still insufficient published data available on the influence of incorporated particles on the quality of composites, *i.e.* on their mechanical, electrical and corrosion properties, while part of the reported data are still controversial.

In this context, the aim of this work is to provide more information about the electrolytic codeposition of alumina nano-powders with copper on a steel substrate, in order to prove the influence of the particles' nature on the corrosion behavior of the composite coatings. The corrosion behavior of the two different types of Al_2O_3 -copper nanocomposite coatings was examined using electrochemical investigation methods such as open circuit potential measurements, polarization measurements, and electrochemical impedance spectroscopy. The electrochemical results were corroborated with those obtained by SEM and EDX investigations.

Experimental conditions

Materials

The tested Al_2O_3 powders commercially available were purchased from Aldrich (544833-50G, $d < 100$ nm) and Escil (A3, $d = 0.3$ μm). CuSO_4 (Prolabo, Paris, France), and H_2SO_4 (Merck, Darmstadt, Germany) were used in the plating bath. All other reagents were of analytical grade and were used without further purification.

Methods

Potentiodynamic polarization measurements were conducted using an electrochemical analyzer

(PARSTAT 2273, USA) connected to a PC for potential control and data acquisition.

The electrochemical experiments were performed in a three-electrode cell with a separate compartment for the reference electrode connected with the main compartment *via* a Luggin capillary. The working electrode was a steel (OL 37) disc, the reference electrode was an $\text{Ag}/\text{AgCl}/\text{KCl}_s$ electrode and the counter electrode was a platinum foil.

Cu and $\text{Cu}-\text{Al}_2\text{O}_3$ films were galvanostatically co-deposited on steel substrate ($S = 0.78$ cm^2) from solutions containing 120 g L^{-1} CuSO_4 and 120 g L^{-1} H_2SO_4 without or with the addition of 20 g L^{-1} Al_2O_3 , at a current density of 25 mA cm^{-2} , during 20 minutes, under magnetic stirring (200 rpm). Prior to use, the working electrode surface was mechanically polished using grit paper of 1200 and alumina powder (0.05 μm), cleaned by ultrasonication and rinsed thoroughly with distilled water.

Corrosion experiments were carried out in 0.2 g L^{-1} aerated Na_2SO_4 solution (pH 3), at room temperature. Open-circuit potential (*ocp*) measurements were performed as a function of time. Anodic and cathodic polarization curves were recorded in a potential range of $E = E_{\text{corr}} \pm 200$ mV for kinetic parameters determination, with a scan rate of 0.25 mV s^{-1} . Impedance measurements were performed at the open-circuit potential in the moment of immersion of the samples into the Na_2SO_4 solution during 48 h from this moment. The impedance spectra were acquired in the frequency range 100 kHz to 10 mHz at 5 points per hertz decade with an AC voltage amplitude of ± 10 mV. The impedance data were then analyzed with software based on a Simplex parameter regression.

Surface analysis used a LEICA S 440 scanning electron microscope with an attached energy dispersive X-ray analyzer. The alumina weight percentage was determined by calculating the average value of four randomly chosen points on the sample surface. Alumina concentration was determined by the stoichiometric ratio of oxygen to aluminum.

Results and discussion

Electrodeposition

As can be seen on the polarization curves recorded during electrodeposition of copper and composite $\text{Cu}-\text{Al}_2\text{O}_3$ coatings (Fig. 1), no significant changes were observed in the kinetically controlled region of the curves, while an inhibition of the current density was noticed in the mixed-controlled region in the presence of Al_2O_3 Aldrich nanoparticles.

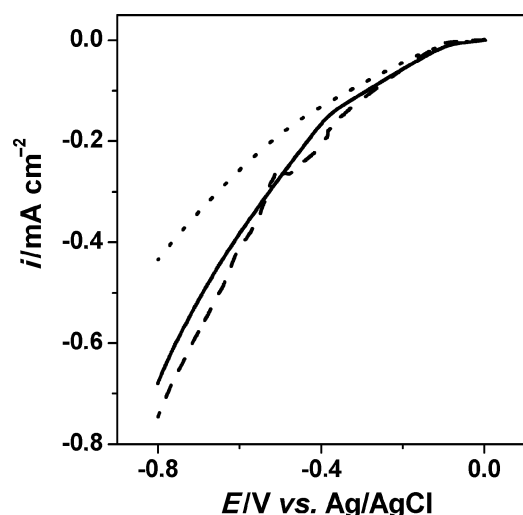


Fig. 1 – Polarization curves obtained during copper electrodeposition in the absence (—) and in the presence of Al_2O_3 Escil ($d = 0.3 \mu\text{m}$) (---) and Al_2O_3 Aldrich ($d < 100 \text{nm}$) (.....) nanoparticles ($i = 25 \text{mA cm}^{-2}$, magnetic stirring 200 rpm)

The decrease of the current density observed at higher polarization in the presence of the Al_2O_3 ($d < 100 \text{nm}$, Aldrich) nanoparticles could be related to a reduction of the electrochemically active area due to the inclusion of the nonconductive Al_2O_3 in the copper deposit. However, the decrease of apparent surface area by entrapment of blocking particles cannot explain the effect occurring in the presence of Al_2O_3 Escil. Other effects, such an enhancement or catalytic phenomenon due to defects and dislocations or chemical heterogeneities generated in the metallic matrix by the embedded particles could also be governing the copper electrodeposition rate.²⁹

The impedance spectra recorded during electrodeposition at different potentials exhibit two capacitive loops and an inductive loop (Fig. 2) and, as expected, present similarities with the impedance spectra previously reported for pure copper electrodeposition.³⁰ No significant modification of the shape, type and number of the loops were observed in the investigated potential region for different values of *d.c.* potential and in the presence of Al_2O_3 , but variations of the apex frequency and of the loops diameter are evident.

The reduction of Cu^{2+} ions adsorbed on alumina was proven to be rate-determining for the codeposition, as it produces real contact between the particle and the cathode.³¹ Thus, the decrease of the charge-transfer resistance values in the presence of Al_2O_3 could be due to an increase of copper ions concentration at the interface, because of their adsorption on the nanoparticles that reach the cathode.

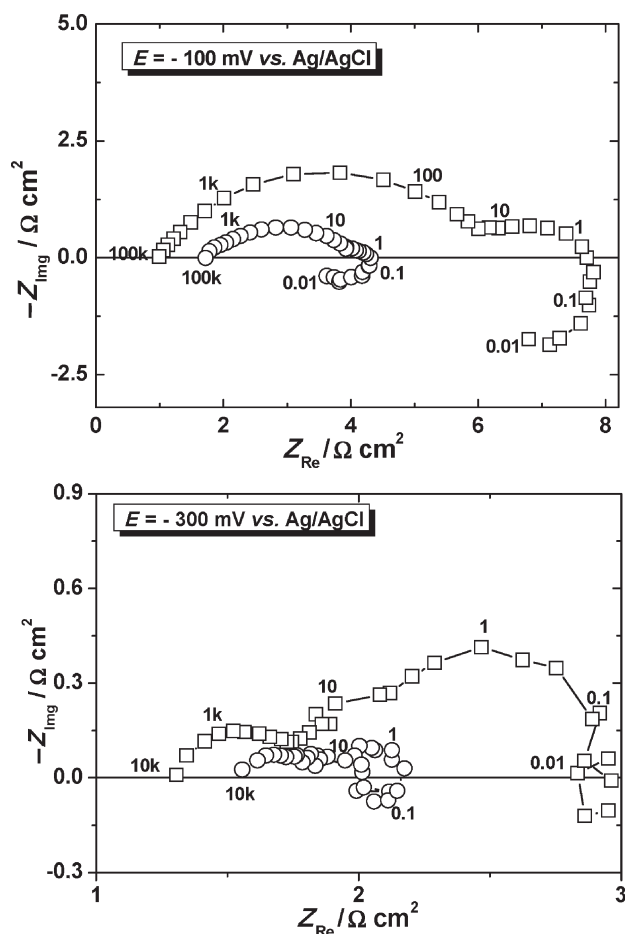


Fig. 2 – Nyquist diagrams obtained at different values of *d.c.* potential, in the absence (\square) and in the presence of Al_2O_3 Aldrich nanoparticles (\circ) during electrodeposition. Frequencies are in Hz.

Morphological and structural analysis

The morphology of the electrodeposited pure copper and of the copper-alumina composite coatings is presented in Fig. 3.

As it may be observed, the morphology changes when particles are added to the electrolyte. The composite deposits obtained in the presence of oxide nanoparticles contain much smaller crystals (b, c) than in the case of pure copper deposit (a). This is because the nanoparticles influence the competitive formation of metal nuclei and crystal growth.³² The alumina nanoparticles disturb the regular growth of copper crystals and cause new nucleation sites to appear.

The incorporation of Al_2O_3 nanoparticles in the deposit was proven by EDX analysis (Fig. 4).

In spite of the fact that the alumina content in the deposit obtained with Al_2O_3 Escil is relatively weak (0.41 weight % Al and 0.95 atomic % Al cor-

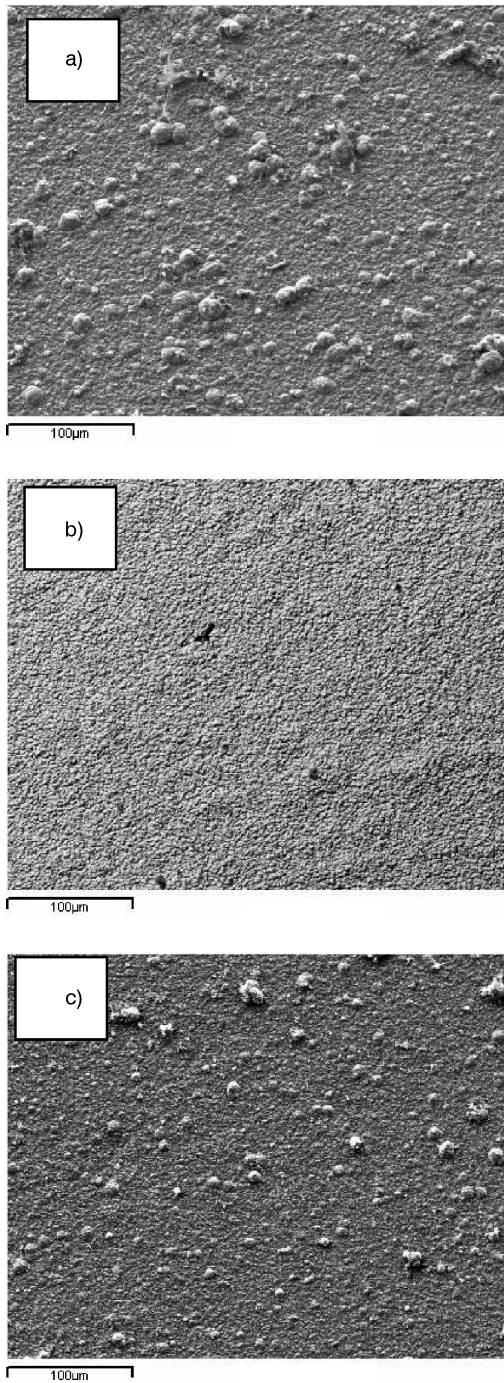


Fig. 3 – SEM micrographs of Cu (a), Cu–Al₂O₃ Escil (b) and Cu–Al₂O₃ Aldrich (c) coatings obtained from a 20 g L⁻¹ particle loading. Experimental conditions: electrolyte 120 g L⁻¹ CuSO₄ and 120 g L⁻¹ H₂SO₄; deposition current density $i = 25 \text{ mA cm}^{-2}$, deposition time 20 minutes, magnetic stirring 200 rpm.

responding to 0.77 weight % Al₂O₃), its effect on the morphology and structure of the deposit is evident. The alumina content is even smaller in the case of Al₂O₃ Aldrich (0.15 weight % Al and 0.35 atomic % Al, corresponding to 0.28 weight % Al₂O₃). However, these values are similar to those reported in the literature.³³

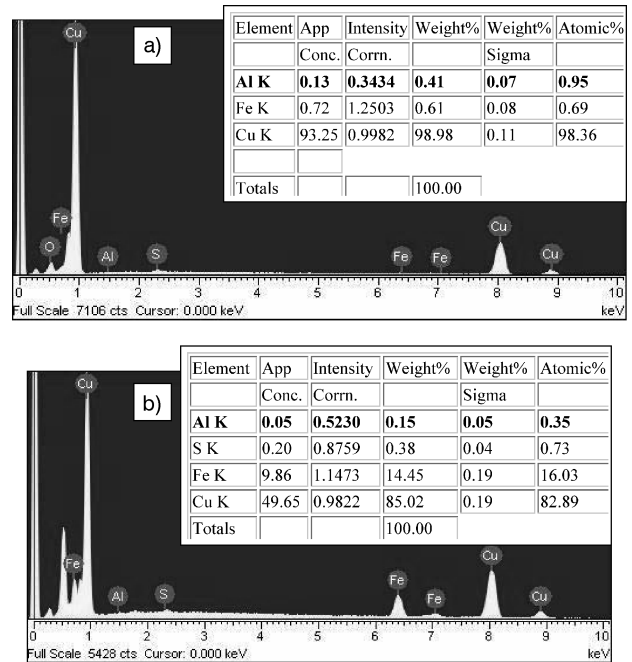


Fig. 4 – EDX spectra of composite coating Cu–Al₂O₃ Escil (a) and Aldrich (b) on steel

In an attempt to explain the different incorporation degree of the two types of alumina powders, their crystalline structure was determined by X-ray analysis. It was found that both alumina powders are mixtures of α and γ Al₂O₃ (results not shown), only the ratio between the two phases was slightly different.

In these conditions, the different particle size of alumina powders was taken into consideration. As already reported in the literature for Ni–Al₂O₃ codeposition,³⁴ increasing the particle size can result, sometimes, in an increase in the amount of incorporation. In our case, Escil alumina having larger particles (0.03 μm) was embedded in higher percent than Aldrich alumina nanopowder (<100 nm). Nevertheless, there are many other factors influencing the inclusion of the particles in the coatings, *i.e.* their surface properties (charge, hydrophilicity/hydrophobicity), the experimental conditions (current density, hydrodynamic conditions) etc. that should be considered.³⁵

Electrochemical corrosion measurements

Open-circuit potential measurements

The open-circuit potentials (*ocp*) evolution in time for OL 37/Cu and OL 37/Cu–Al₂O₃ electrodes recorded after their immersion in Na₂SO₄ solution (pH 3) is presented in Fig. 5.

For all electrodes, the *ocp* values gradually increase in the negative direction during the first min-

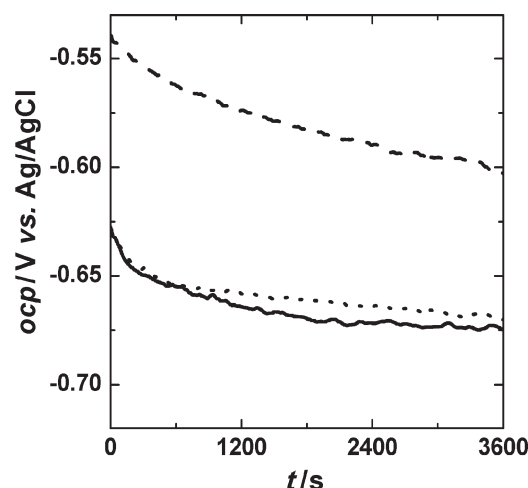


Fig. 5 – Evolution of open circuit potentials for OL 37/Cu (—), OL 37/Cu–Al₂O₃ Escil (---) and OL 37/Cu–Al₂O₃ Aldrich (.....) electrodes immersed in 0.2 g L⁻¹ Na₂SO₄ (pH 3)

utes to reach a stationary state characterized by -0.600 V vs. Ag/AgCl in the case of alumina Escil and of -0.670 V vs. Ag/AgCl in the case of alumina Aldrich. This evolution of the potential toward more negative values with the increase of immersion time is due to the formation of a corrosion product layer. According to this growth, the cathodic reaction is hindered and consequently the corrosion potential becomes more negative.³⁶

The *ocp* value is almost the same for OL 37/Cu–Al₂O₃ Aldrich and for OL 37/Cu electrodes. Contrarily, in the case of Cu–Al₂O₃ Escil coatings, a shift of the *ocp* towards more positive potentials is observed, suggesting a more noble character of the Cu–Al₂O₃ coating, associated with an inhibition of the anodic reaction and, consequently, with stronger corrosion resistance.

Potentiodynamic polarization measurements

The cathodic and anodic polarization curves of OL 37/Cu and OL 37/Cu–Al₂O₃ electrodes recorded immediately after their immersion in Na₂SO₄ solution (pH 3), and after 24 h are shown in Fig. 6.

In the first moments after the immersion in the Na₂SO₄ solution, both composite coatings had similar behavior: the corrosion potential is more positive than that of pure copper. After 24 h, only the corrosion potential of the Cu–Al₂O₃ Escil remains more positive and in this case, the corrosion current strongly decreases.

As it can be seen, the results are consistent with the values recorded for the *ocp* potentials, pointing to a stronger effect on the corrosive properties of the composite coating in the case of Al₂O₃ Escil than in the case of Al₂O₃ Aldrich. This behavior may be because the particles of the non-con-

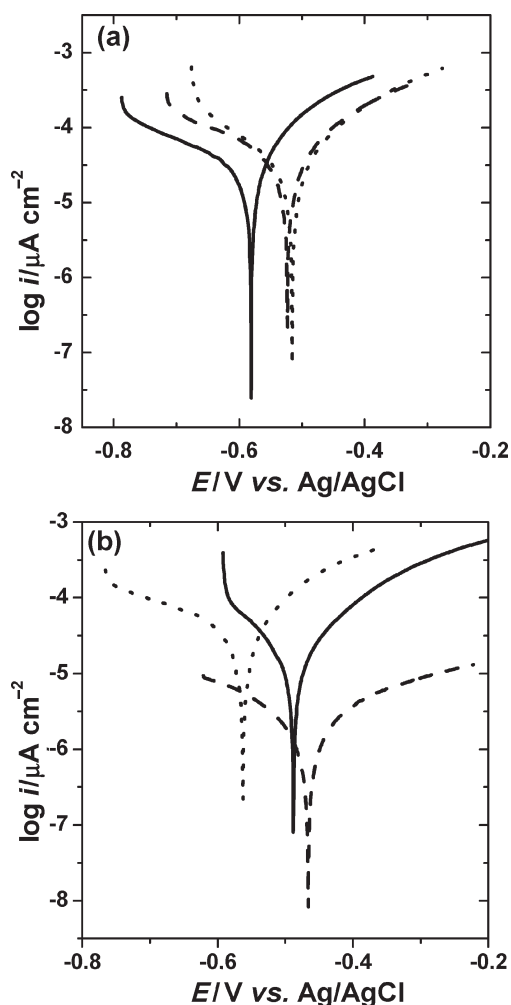


Fig. 6 – Polarization curves for OL 37/Cu (—), OL 37/Cu–Al₂O₃ Escil (---) and OL 37/Cu–Al₂O₃ Aldrich (.....) electrodes in 0.2 g L⁻¹ Na₂SO₄ (pH = 3) at the immersion moment (a) and after 24 hours (b)

ducting aluminum oxide, with high chemical resistance can have a screening effect, and since they are highly dispersed in the metallic coating, they reduce the area of contact between the metal matrix and the corroding medium. This effect is more pronounced in the case of Cu–Al₂O₃ Escil than in the case of Cu–Al₂O₃ Aldrich, due to the higher incorporation fraction of the first one. However, the effect of particle content in the composite coatings on the deposit properties depends not only on the amount of the particles embedded in the metal matrix, but more importantly, on the size and distribution of the particles in the metal matrix.³⁷

According to the Stern-Geary theory,³⁸ the current density i near to the open-circuit potential can be expressed by the following equation:

$$i = i_{\text{corr}} \{ \exp[b_a (E - E_{\text{corr}})] - \exp[b_c (E - E_{\text{corr}})] \} \quad (1)$$

where b_a and b_c are the anodic and cathodic activation coefficients, respectively.

Table 1 – Kinetic parameters of the corrosion process obtained by regression using the Stearn-Geary equation for interpretation of the polarization curves

Electrode	Immersion time / h	$E_{\text{corr}}/\text{V vs. Ag/AgCl}$	$i_{\text{corr}}/\mu\text{A cm}^{-2}$	b_a/V^{-1}	$-b_c/\text{V}^{-1}$
OL 37/Cu	0	-0.588	75.0 ± 2.40	11.5 ± 0.18	2.14 ± 0.18
	24	-0.488	79.4 ± 3.12	7.16 ± 0.11	3.9 ± 0.40
OL 37/Cu–Al ₂ O ₃ Aldrich	0	-0.516	86.5 ± 1.02	8.9 ± 0.05	4.12 ± 0.08
	24	-0.562	47.7 ± 1.24	16.2 ± 0.30	5.3 ± 0.20
OL 37/Cu–Al ₂ O ₃ Escil	0	-0.530	94.6 ± 0.27	7.4 ± 0.11	4.0 ± 0.15
	24	-0.470	4.8 ± 0.01	4.5 ± 0.21	5.97 ± 0.1

Therefore, the values of E_{corr} and the corrosion current density (i_{corr}) were evaluated by a non-linear regression calculation at near zero overall current. The values of the corrosion parameters in the absence and presence of Al₂O₃ in the deposit, calculated from the polarization curves are presented in Table 1.

In all cases, the correlation factor R^2 varies between 0.9937 and 0.9995 indicating a good fitting result. The confident interval for i_{corr} was in the order of one percent whereas E_{corr} was determined with an error margin lower than 1 mV.

As can be seen from Table 1, the values of the Tafel coefficients in the presence of Al₂O₃ change in comparison with pure copper, which indicates that the alumina particles influence the kinetics of both the anodic and cathodic processes. The difference between the values of the kinetic parameters corresponding to the two types of composite coatings could be explained, as mentioned before, by the different incorporation fraction, grain size and crystalline structure of the incorporated alumina powders, which may influence the corrosion behavior of the resulting composite coating.

Electrochemical impedance spectroscopy

The impedance spectra recorded at *ocp* in the absence and presence of Al₂O₃ nanoparticles in the copper coatings (Fig. 7) exhibit a predominant capacitive behavior with depressed loops.

As can be seen from Fig. 7, at the beginning, the polarization resistance, R_p , corresponding to the lower frequency limit of the impedance spectra, increases with increasing of immersion time. The changes of the impedance values with increasing immersion time show that a barrier related to the formation of corrosion products gradually forms on the copper surface. An increase of R_p could be explained by a limitation of the active area by this layer, more important when the layer is more developed (thicker and/or more compact).³⁶ This phe-

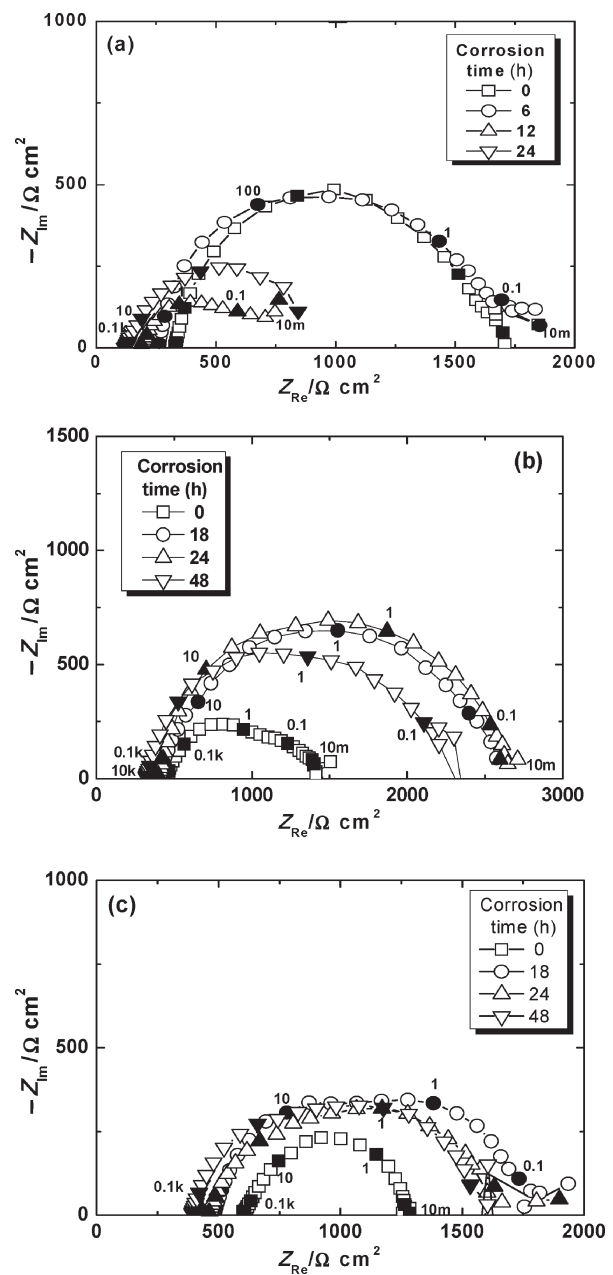


Fig. 7 – EIS evolution for OL 37/Cu (a), OL 37/Cu–Al₂O₃ Escil (b) and OL 37/Cu–Al₂O₃ Aldrich (c) electrodes immersed in $0.2 \text{ g L}^{-1} \text{ Na}_2\text{SO}_4$ ($\text{pH} = 3$) solution

nomenon has been noticed both in the case of pure copper and in the case of the composite coatings, suggesting an evolution of the corrosion products layer in time. Further work will address the chemical composition of these layers. Although not clearly seen in Fig. 7, it was found that the impedance results could be suitably simulated to properly reproduce the experimental data by using two time constants under capacitive relaxation. Therefore, the (2RC) electrical equivalent circuit presented in Fig. 8 was adopted to carry out the non-linear regression calculation with a Simplex method.³⁹

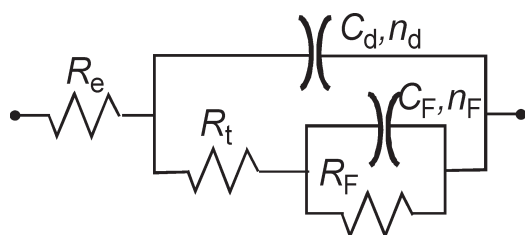


Fig. 8 – The (2RC) equivalent electrical circuit used for computer fitting of the experimental data

In the circuit from Fig. 8, R_e represents the electrolyte resistance; R_t and C_d correspond to the charge-transfer resistance and to the double layer

capacitance at the copper/electrolyte interface, while R_F and C_F symbolize the faradic resistance and faradic capacitance due to an oxidation – reduction process taking place at the electrode surface, probably involving the corrosion products. The parameters n_d and n_F are coefficients representing the depressed characteristic of the two capacitive loops in the Nyquist diagrams.

The values of the impedance parameters calculated by non-linear regression of the impedance data in the absence and presence of Al_2O_3 in the coatings are presented in Table 2.

After 24 h, larger values of the charge-transfer resistance and smaller values of double layer capacitances were noticed in the case of both composite coatings, suggesting the formation of a barrier of corrosion products that hindered further evolution of the corrosion process. This was confirmed also by the large values of polarization resistances in the case of these coatings.

In the case of pure copper, the values of the charge-transfer resistance R_t indicate that the layer of corrosion products is not very compact. R_t decreases systematically, while C_d increases, proving an increase of surface roughness due to the formation of a non-protective corrosion layer in parallel with the facilitation of the corrosion process.

Table 2 – Parameter values for corrosion of OL37/Cu and different OL37/Cu– Al_2O_3 coatings, calculated by non-linear regression of the impedance data using the equivalent electrical circuit from Fig. 8

Substrate	Immersion time / h	$R_e / \Omega \text{ cm}^2$	$R_t / \Omega \text{ cm}^2$	$C_d / \mu\text{F cm}^{-2}$	$R_F / \Omega \text{ cm}^2$	$C_F / \mu\text{F cm}^{-2}$	$R_p / \Omega \text{ cm}^2$
OL 37/Cu	0	329.7	873.5	17.90	794.8	343	1668.24
	6	258.4	980.8	23.56	774.6	880	1755.37
	12	185.1	524.6	870.69	210.9	2803	735.53
	24	121.4	113.3	1310	704.8	660	818.11
OL 37/Cu– Al_2O_3 Aldrich	0	603.4	150.7	33.04	526.2	67.5	676.85
	12	171.4	247.6	24.82	798.4	202	1046.09
	18	454	685.8	53.60	564.2	328.5	1249.95
	24	393	700	37.17	494.6	436.5	1194.65
	48	387	360.1	345.09	560	2050	920.09
OL 37/Cu– Al_2O_3 Escil	1	451.3	687.5	7.75	294	540.5	981.61
	18	405.6	1016.1	29.32	1179.7	73.60	2195.80
	24	396.3	1681	22.9	612	404.7	2293.07
	48	333	1166.5	34.8	930	422.8	2096.52

* $R_p = R_t + R_F$

In the case of Cu–Al₂O₃ Escil, the general tendency of R_t was to increase, suggesting the formation of a more compact corrosion products layer, that hinders the charge transfer at the interface.

For the composite coatings, the polarization resistance, R_p increased with the immersion time, until it attained, after 18 hours, a value that remained almost constant throughout the period covered by the present experiments. This indicated a relative stabilization of the corrosion products layer.

After 48 h, an apparent decrease of the charge-transfer resistance R_t in time was observed. This variation could be due to an increase of the electrode roughness that counterbalances the lowering of the surface area of the electrode by embedded particles²⁹ or to a damage of the corrosion products layer.

As it can be seen from the comparison of the calculated and experimental impedance spectra presented in Fig. 9, the (2RC) equivalent electrical circuit reproduces suitably the experimental data ob-

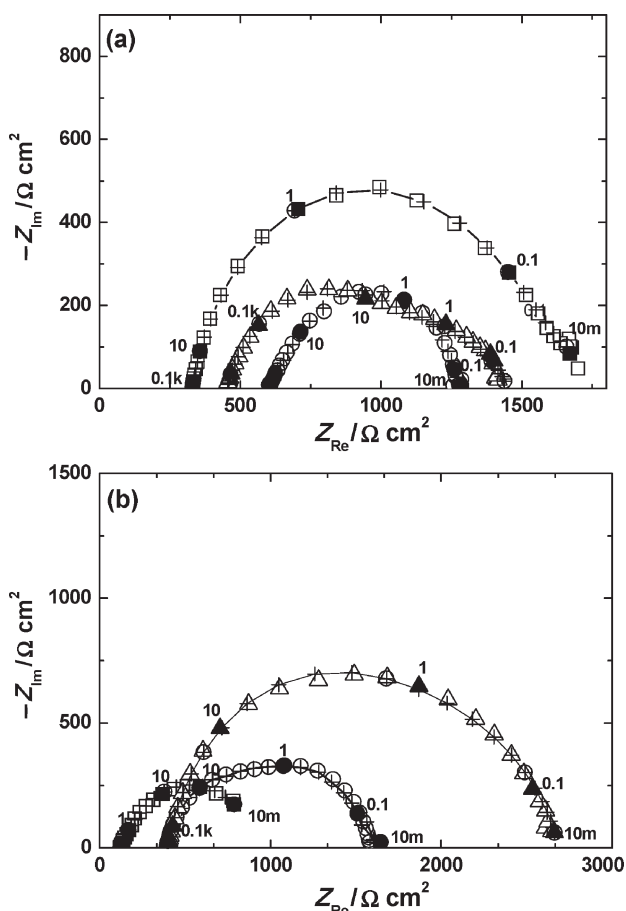


Fig. 9 – Experimental and simulated impedance diagrams for OL 37/Cu (\square) OL 37/Cu–Al₂O₃ Escil (\triangle) and OL 37/Cu–Al₂O₃ Aldrich (\circ) coatings in 0.2 g L⁻¹ Na₂SO₄ (pH = 3) at the immersion moment (a) and after 24 hours (b). The symbol (–+–) corresponds to the fitted data. Frequencies are expressed in Hz.

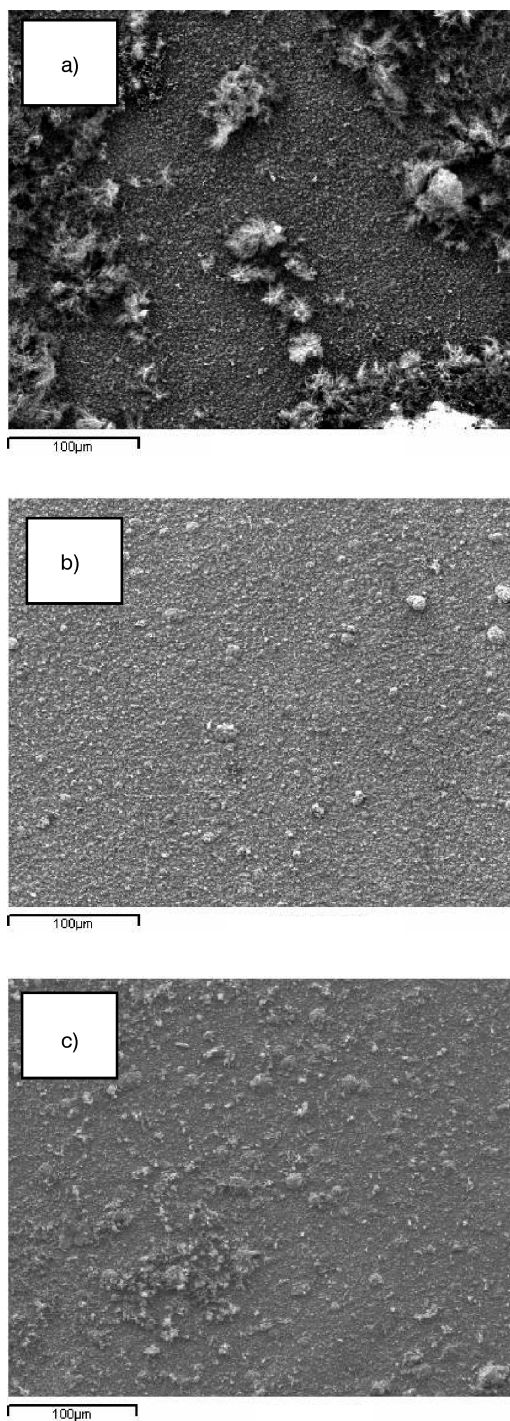


Fig. 10 – SEM micrographs of OL 37/Cu (a), OL 37/Cu–Al₂O₃ Escil (b) and OL 37/Cu–Al₂O₃ Aldrich (c) coatings after 24 hours of immersion in 0.2 g L⁻¹ Na₂SO₄ (pH 3)

tained both in the absence and presence of different incorporated alumina nanoparticles.

The behavior of the composite layers was confirmed by the SEM micrographs taken after 24 hours of immersion (Fig. 10). As can be observed, the most corroded is the pure copper surface, followed by Cu–Al₂O₃ Aldrich and Cu–Al₂O₃ Escil composite coatings.

Conclusions

The analysis of the results led to the following conclusions:

i) The wt % of incorporated alumina is similar with that reported in the literature. In spite of the low incorporation fraction, all the electrochemical measurements showed that the corrosion process on Cu–Al₂O₃ composite surfaces was slower than on pure copper surface.

ii) Al₂O₃ Escil incorporates better and confers better corrosion protection to the copper coatings than Al₂O₃ Aldrich. The particles dimensions could be one of the reasons for this behavior, but probably not the only one.

iii) All the electrochemical measurements showed that the corrosion process on Cu–Al₂O₃ composite surface was slower than on pure copper surface.

iv) Further investigations are necessary to elucidate the role of the properties (charge, hydrophilicity/hydrophobicity etc.) of Al₂O₃ nanoparticles on the corrosion behavior of the Cu–Al₂O₃ composite coatings.

ACKNOWLEDGEMENTS

The authors thank Dr. Georges Maurin (“Pierre et Marie Curie” University, LISE, Paris, France), and Prof. Dr. Pop Aurel (“Babes-Bolyai” University, Faculty of Physics, Cluj-Napoca, Romania) for X-ray diffraction analysis of alumina powders. The financial support within the projects PN II INOVARE No. 97/28.09.2007 and CNCSIS-A 1469/2008 is gratefully acknowledged.

The authors address special thanks to Dr. Hisasi Takenouti (“Pierre et Marie Curie” University, LISE Paris, France) for sharing with them the know-how of the impedance diagrams simulation method.

List of symbols

- i – current density, A m⁻²
 i_{corr} – corrosion current density, A m⁻²
 E – potential, V
 E_{corr} – corrosion potential, V
 ocp – open-circuit potential, V
 b_a – anodic activation coefficient, V⁻¹
 b_c – cathodic activation coefficient, V⁻¹
 R_e – electrolyte resistance, Ω m²
 C_d – double layer capacitance at the copper/electrolyte interface, F m⁻²
 R_t – charge transfer resistance, Ω m²

- n_d – constant phase element coefficient associated with the double layer capacitance
 C_F – faradic capacitance due to an oxidation – reduction process taking place at the electrode surface, probable involving the corrosion products, F m⁻²
 R_F – faradic resistance of the corrosion products accumulated at the interface, Ω m²
 n_F – constant phase element coefficient associated with the faradic capacitance
 R_p – polarization resistance, Ω m²
 Z – impedance, Ω m²
 t – time, s

References

- Musiani, M., *Electrochim. Acta* **45** (2000) 3397.
- Bund, A., Thieming, D., *J. Appl. Electrochem.* **37** (2007) 345.
- Wu, J. Y., Zhou, Y. C., Wang, J. Y., *Mat. Sci. Eng.* **422** (2006) 266.
- Szczygiel, B., Kolodziej, M., *Electrochim. Acta* **50** (2005) 4188.
- Chen, L., Wang, L., Zeng, Z., Zhang, J., *Mat. Sci. Eng.* **434** (2006) 319.
- Bin-shi, X., Hai-dou, W., Shi-yun, D., Bin, J., Wei-yi, T., *Electrochem. Comm.* **7** (2005) 572.
- Boskovic, I., Mentus, S. V., Pjescic, M., *Electrochim. Acta* **51** (2006) 2793.
- Banerjee, S., Chakravorty, D., *J. Appl. Physics* **85** (1999) 3623.
- Armelo, L., Barreca, D., Bottaro, G., Gosparotto, A., Gross, S., Maragno, C., Tondello, E., *Coord. Chem. Rev.* **250** (2006) 1294.
- Tuaweri, T. J., Wilcox, G. D., *Surf. Coat. Tech.* **200** (2006) 5921.
- Shi, L., Li, Y., Xue, C., Zhuang, H., He, J., Tian, D., *Appl. Surf. Sci.* **252** (2006) 2853.
- Chen, L., Wang, L., Zeng, Z., Xu, T., *Surf. Coat. Tech.* **201** (2006) 599.
- Tu, W., Xu, B., Dong, S., Wang, H., *Mat. Lett.* **60** (2006) 1247.
- Nowak, P., Socha, R. P., Kaisheva, M., Fransær, J., Celis, J. P., Stoinov, Z., *J. Appl. Electrochem.* **30** (2000) 429.
- Zhu, J., Liu, L., Zhao, H., Shen, B., Hu, W., *Materials and Design* **28** (2006) 1958.
- Xiao-Hong, Y., Yong-bing, L., Qi-fei, S., Jian, A., *Trans. Nonferrous Metals Soc. China* **16** (2006) s1.
- Balaji, R., Pushpavanam, M., Kumar, K. Y., Subramanian, K., *Surf. Coat. Tech.* **201** (2006) 3205.
- Popov, K. I., Djokic, S. S., Grgur, B. N., *Fundamental Aspects of Electrometallurgy*, Kluwer Academic/Plenum Publ., New York, 2002, pp. 121.
- Baohong, T., Ping, L., Kexing, S., Yan, L., Yong, L., Fengzhang, R., Juanhua, S., *Mat. Sci. Eng. A* **435–436** (2006) 705.
- Stojak, J. L., Talbot, J. B., *J. Appl. Electrochim.* **31** (2001) 559.
- Chen, E. S., Lakshminarayanan, G. R., Sautter, F. K., *Metallurgical Trans.* **2** (1971) 937.
- Celis, J. P., Kelchtermans, H., Roos, J. R., *Trans. Inst. Met. Finish.* **56** (1978) 41.
- Roos, J. R., Celis, J. P., Kelchtermans, H., *Thin Solid Films* **54** (1978) 173.

24. Findik, F., Uzum, H., *Mater. Design* **24** (2003) 489.
25. Shi, Z., Yan, M., *Appl. Surf. Sci.* **134** (1998) 103.
26. Oh, S.-T., Sekino, T., Niihara, K., *Nanostruct. Mater.* **10** (1998) 715.
27. Slade, P. G., *IEEE Trans. Compon. Hybrids Manuf. Technol.* **9** (1986) 3.
28. Celis, J. P., Ross, J. R., *J. Electrochem. Soc.* **124** (1977) 1508.
29. Lozano-Morales, A., Podlaha, E. J., *J. Electrochem. Soc.* **151** (2004) C478.
30. Varvara, S., Muresan, L., Popescu, I. C., Maurin, G., *J. Appl. Electrochem.* **33** (2003) 685.
31. Roos, J. R., Celis, J. P., Helsen, J. A., *Trans. Inst. Met. Finish.* **55** (1977) 113.
32. Benea, L., Bonora, P.-L., Borello, A., Martelli, S., *Wear* **249** (10–11) (2002) 995.
33. Stojak, J. L., Fransaer J., Talbot J. B., Review of Electrocodeposition in *Alkire, R. C., Kolb, D. M.* (Eds.), *Advances in Electrochemical Science and Engineering*, Vol. 7, Wiley-VCH Verlag GmbH, 2001, pp. 193–223.
34. Shao, I., Vereecken, P. M., Cammarata, R. C., Searson, P. C., *J. Electrochem. Soc.* **149** (2002) C610-C614.
35. Bund, A., Thiemig, D., *J. Appl. Electrochem.* **37** (2007) 345.
36. Bousselmi, L., Fiaud, C., Tribollet, B., Triki, E., *Corr. Sci.* **39** (1997) 1711.
37. Wang, W., Hu, F. Y., Wang, H., Guo, H.-T., *Scripta Materialia* **53** (2005) 613.
38. Stern, M., Geary, A. L., *J. Electrochem. Soc.* **104** (1957) 56.
39. Trachli, B., Keddam, M., Shrir, A., Takenouti, H., *Corr. Sci.* **44** (2002) 997.